Available online at www.sciencedirect.com
ScienceDirect
Journal of Power Sources 182 (2008) 400–412
JOURNAL OF POWER SOURCES
www.elsevier.com/locate/jpowsour

Fundamental mechanisms limiting solid oxide fuel cell durability

Harumi Yokokawa [a,*], Hengyong Tu [b], Boris Iwanschitz [c], Andreas Mai [c]

[a] *National Institute of Advanced Industrial Science and Technology (AIST), Higashi 1-1-1, Tsukuba, Ibaraki 305-8565, Japan*
[b] *Institute of Fuel Cell, Department of Automation, School of Electronic Information and Electrical Engineering, Shanghai Jiao Tong University, 1954 Hua Shan Road, Shanghai 200030, China*
[c] *Hexis AG, Hegifeldstrasse 30, CH-8404 Winterthur, Switzerland*

Received 1 December 2007; received in revised form 16 January 2008; accepted 6 February 2008
Available online 17 February 2008

Abstract

The fundamental issues associated with solid oxide fuel cell (SOFC) durability have been reviewed with an emphasis on general features in SOFCs and respective anode and cathode related phenomena. As general features, physicochemical properties and cell performance degradation/failure are correlated and bridged by the electrode reaction mechanisms. Particular emphasis is placed on the elemental behaviour of gaseous impurities and the possible role of liquids formed from gaseous substances. The lifetime of a state-of-the-art Ni cermet anodes is limited by a variety of microstructural changes, which mainly result from material transport-, deactivation- and thermomechanical mechanisms. Anode degradation can mainly be influenced by processing, conceptual and operating parameters. Designing a redox stable anode is currently one of the biggest challenges for small scale SOFC systems. Degradation mechanisms of different cathode materials are reviewed with a focus on the intrinsic degradation of doped lanthanum manganites (e.g. LSM) and doped lanthanum ferro-cobaltites (LSCF). Manganese-based perovskites can be regarded to be sufficiently stable, while for the better performing LSCF cathodes some intrinsic degradation was detected. New materials that are supposed to combine a better stability and high performance are also shortly mentioned.

Keywords: Solid oxide fuel cell; Degradation; Durability; Cathode; Anode; Impurities

1. Introduction

Solid oxide fuel cells (SOFCs) offer great promise as a clean and efficient process for directly converting chemical energy to electricity while providing significant environmental benefits [1,2]. SOFCs can reach electrical efficiencies of 45–50% [3]. Due to their high operating temperatures, cogeneration of heat and power can be effectively employed with total efficiency of more than 80%. SOFC cell elements are constructed from ceramic materials. The raw ingredients for these ceramics are relatively inexpensive. Due to the high operating temperature of SOFCs, the need for expensive precious metal catalysts is negligible. SOFCs are unique in a sense that they can run on a wide range of fuels, including natural gas, biogas, diesel, LPG, methanol, DME and ethanol. Hydrogen-rich gases containing carbon monoxide do not need to undergo additional "gas clean-up" steps. Thus, they have the ability to operate within both the current fossil fuel-based energy infrastructure and the future proposed hydrogen fuel infrastructure.

Besides costs and performance, long-term stability is an important requirement for the commercial application of the SOFC technology. For stationary applications, the commercial lifetime requirement is generally more than 40,000 h. In comparison, up to a 20,000 h lifetime with more frequent thermal cycles is required for auxiliary power units in transportation applications. However, these lifetime requirements have not been met yet. Operating conditions of SOFCs lead to a variety of degradation mechanisms and represent a significant challenge in meeting lifetime requirements. For the stationary applications, the chemical instability at the interfaces is one of the key issues, whereas the thermomechanical instability is important in the transportation applications because of frequent thermal cycles [2]. It is therefore essential to increase the understanding in the degradation mechanisms for these issues. Thus, great efforts have been made in analyzing SOFC degradation mechanism worldwide. The total degradation of the stack performance originates from

* Corresponding author. Tel.: +81 29 861 4542; fax: +81 29 861 4540.
E-mail address: h-yokokawa@aist.go.jp (H. Yokokawa).

0378-7753/$ – see front matter © 2008 Elsevier B.V. All rights reserved.
doi:10.1016/j.jpowsour.2008.02.016

the deterioration of the sole components as well as from the mutual interactions among the cell components. Degradation mechanisms originated from the cell components include, for example, the decrease in the intrinsic electrical conductivity of stabilized zirconia electrolyte [4], coarsening of nickel particles and carbon deposition in the anode [5–7]. Furthermore, compatibility of cathode and electrolyte interfaces has been an important issue [8] and even in a recent cathode material, enrichment of the Sr component was detected at the cathode–electrolyte and cathode–current collector interfaces leading to an increase of interface resistivities [9,10]. At a stack level, degradation mechanisms include poisoning of the cathode by gaseous Cr species from metallic interconnects [10–13] and chemical interactions between glass–ceramic sealants and ferritic steel interconnects [14]. Furthermore, various cycling conditions such as thermal cycle, redox cycle, and load cycle also impact constituent stability of SOFCs [15–17]. It is therefore necessary to develop improved materials and processes etc. to mitigate such mechanisms. Quite recently, impact of impurities has been also reported in a stack/system level after a long-term operation [18].

In the present article, the general features of chemical reactions and related phenomena leading to mechanical instability or electrode performance degradation are first described in details. Then degradation mechanisms in anode and cathode are extensively discussed for their respective issues.

2. General features of SOFC materials behaviour associated with degradation issues

In order to discuss degradation of SOFC performance, it is essential to realize that the SOFC stack development has some technological difficulties, because SOFC stacks consist of all ceramic solid materials except for several metal components [2]. This makes it necessary to develop simultaneously materials, materials processing and stack design under a specified application concept. First break through in SOFC stack development was achieved by Westinghouse in 1980s with developments of so-called first generation materials such as YSZ electrolyte, lanthanum strontium manganite cathode, Ni anode and $LaCrO_3$-based oxide interconnects, application of electrochemical vapour deposition (EVD) process and invention of sealless tubular design [3]. Since then, many proposals have been made on materials selection, adoption of inexpensive processing, and alternative stack design. Since degradation is deeply associated with the specified materials, fabrication methods, and stack designs, there should be many R&D fronts associated with degradation for such stacks. For example, we should recognize that the sealless tubular cell/stack confirmed extremely low degradation, namely 0.1% per 1000 h^{-1}, during more than 70,000 h [3]. On the other hand, recent rapid progress in the intermediate temperature SOFCs has achieved a comparative efficiency as the tubular stacks, even for a small system of 1 kW, while degradations in IT SOFCs are in general worse than for the sealless tubular stacks because more active cathodes and inexpensive but less stable metal interconnects are used.

In this section, generalized features of degradation will be discussed from the physicochemical point of view. A basic idea is illustrated in Fig. 1. Degradation is usually defined as the performance degradation as well as mechanical failure such as crack formation and propagation. Systematic investigations of such degradation phenomena are carried out with several tests; durability test, thermal cycle tests and redox stability tests but also accelerated life time tests. To predict the lifetime of a stack, it is essential to understand the physicochemical reasons for respective degradations. For such a purpose, physicochemical features should be clarified in the relation to the electrochemical mechanism. Furthermore, degradation may occur as a result of many related deteriorations which take place sequentially. These deterioration chain phenomena have been well recognized for MCFC but not SOFCs [2], probably because there are many different types of stack designs and related materials. In what follows, the general features of these degradations of SOFC stacks are discussed.

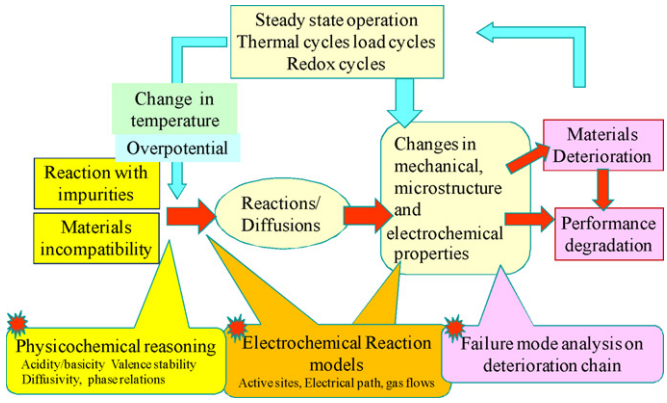

Fig. 1. Schematic description of phenomena associated with cell performance degradation or mechanical instability in high temperature solid oxide fuel cells.

2.1. Physicochemical properties

Chemical changes in cell components generally take place as functions of temperature and oxygen potentials. These properties are determined primarily by selection of cell operation conditions. Such factors affecting the reactivity of cell components can be summarized as follows:

(1) Temperature: temperature dependence is determined in terms mainly of the entropy term, which is governed by a number of gaseous species involved in the chemical reactions; For example, metal carbonate reactions from metal oxide and CO_2 are favoured at lower temperatures [8,19].
(2) When oxygen gas is involved, temperature and oxygen potential become important. Almost all reactions associated with the perovskite-type cathodes with the fluorite-type oxides accompany with the change in valence state of the transition metal ions in the perovskite oxides so that they depend on both temperature and oxygen potential [8,20,21].
(3) In addition, the acid–base relation [23-25] should be considered for chemical reactivity of cell components against impurities in stack materials or in gases. The most important point in SOFCs is that the electrolyte materials consist of rather less acidic and less basic compounds, compared

with MCFC or low temperature PAFC, PEFC, AFC. ZrO_2 is weak acidic compound, while Y_2O_3 is weak basic compound. This chemically mildness of the electrolyte provides the physicochemical basis of obtaining the long life time of, for example, tubular cells. The reaction of LSM and YSZ can be characterized as the rearrangement of combination of acidic and basic components. For example, the following reaction

$$LaMnO_3 + ZrO_2 = 0.5La_2Zr_2O_7 + 0.5Mn_2O_3 \quad (1)$$

can be interpreted in terms of the difference in the acidity of ZrO_2 and Mn_2O_3. For the Y_2O_3 component, the following is a typical acid–base reaction:

$$(ZrO_2)_{0.92}(Y_2O_3)_{0.08} + 0.08V_2O_5 = 0.92ZrO_2(\text{monocl}) + 0.08YVO_4 \quad (2)$$

(4) This also shows that the interaction with gases becomes important in SOFCs. This is because many acidic substances (HCl(l), H_2SO_4(l), H_2CO_3(l), HBO_3, H_3PO_4) at room temperature becomes gaseous species (HCl(g), SO_2(g), CO_2(g), H_3BO_3(g), $CrO_2(OH)_2$(g)) at high temperatures, whereas basic alkali elements also tend to exist as gaseous species such as NaOH(g), KOH(g) etc.
(5) Among oxides used, the SrO component becomes the key basic substance that interacts with acidic substances. As acidic substances, gaseous species such as CO_2, SO_2, $Si(OH)_4$, P_410(g), H_3BO_3(g), $CrO_2(OH)_2$ are important.
(6) Typical gaseous acid–base reactions to form condensed salts contain a change in mole number of gaseous species; for example,

$$SrO(s) + CO_2(g) = SrCO_3(s) \quad (3)$$

This thermodynamic reactivity therefore depends on temperature because of the entropy effect. Since the valence state is quite different among the anode and the cathode atmospheres, the acid–base reactions appear in a quite different manner among both atmospheres; for example in the Na–S–O–H system, Na_2SO_4 is important in air, while Na_2S can be formed in the reducing atmosphere.
(7) Possible sources of contaminations are NaCl in air and $CaSO_4$ (or $SrSO_4$) in water. This leads to the contamination of anodes with Sr and S, and also to the corrosion of metals due to the Na_2SO_4 formation in a post combustion zone.

2.2. Issues in thermodynamic data

The above features strongly depend on the availability of thermodynamic properties and phase relations. Yokokawa et al. started to compile extensively the thermodynamic data of compounds in the multicomponent systems associated with solid oxide fuel cells from late 1980s [26–37] with an aid of correlation [38,39]; they also made thermodynamic analyses on materials issues in SOFCs, namely cathode/electrolyte interface stability [26–28,33], sintering characteristics of $LaCrO_3$-based interconnect [32] and other issues in high temperature electrochemical devices. For this purpose, they also developed the generalized chemical potential diagrams to treat the thermodynamic compatibility of dissimilar materials [40–42]. They successfully provided basis of understanding the interface stability. Their thermodynamic data are available as the thermodynamic database MALT [43].

Even so, their approach was a kind of try and error fitting method to obtain a consistent set of thermodynamic and phase relation data and also they adopted many estimates because the availability of data was limited. Recently, many investigations on the thermodynamic modelling [44,45] have been made by utilizing more advanced computer software package for managing database and evaluating a consistent set among different experimental data such as Thermo-Calc [46]. Furthermore, progress has been also made in experimental determination of the thermodynamic properties. These thermodynamic evaluation procedures usually start with binary systems and extend to higher system [47–54]. In the LSM–YSZ system, these recent evaluated data are essentially the same as those evaluated by Yokokawa except for $La_2Zr_2O_7$ [53] The difference in $La_2Zr_2O_7$ originates from the following considerations:

(1) Yokokawa determined data of $La_2Zr_2O_7$ so as to reproduce the experimental results of diffusion couples between (La, Sr)MnO_3/YSZ by Lau and Singhal [55] and between $LaCoO_3$/YSZ by Echigoya et al. [56] simultaneously. At that time, one calorimetric investigation on $La_2Zr_2O_7$ [57] was available so that evaluation was made within uncertainty of this experimental value.
(2) On the other hand, Chen et al. evaluated data of $La_2Zr_2O_7$ in the ZrO_2–La_2O_3 pseudo binary system by relying on the calorimetric data by Bolech et al. [58].

From this comparison, the following important features can be derived:

(1) Industrial important materials are usually of multicomponent materials and therefore, examination on material compatibility should focus on such complicated systems since experimental information is available in these systems. For example, YSZ is normally used instead of monoclinic ZrO_2 and therefore, compatibility test is made between cathode and YSZ not between cathode and monoclinic ZrO_2. This causes some difficulty in the thermodynamic evaluation. This should start with many binary systems and makes it a long way of obtaining a large set of data which can be compared with experimental data.
(2) The major difference in the evaluated data between Yokokawa's one [26–28] and Chen's one [53,54]should originate from inconsistency among the experimental data. For the present case, the calorimetric values are different in literature. Furthermore, the recent calorimetric value [58] is not consistent with the most important diffusion couple experiment by Lau and Singhal [55]. To resolve such discrepancy, new experimental confirmation should be made

in calorimetry and also in phase relation investigation by changing oxygen partial pressure.

Another features associated with the thermodynamic data are concerning the gaseous species. Thermodynamic data for many gaseous species become available due to the extensive investigation using high temperature mass spectrometry [59,60]. For example, $Si(OH)_4$ becomes available during the investigation of oxidation of SiC with water vapour [61]. Even so, there is still lack in data for double oxide or double salts [22]. It is highly hoped to expand the thermodynamic information to more complicated systems.

2.3. Electrode reaction models

The most important feature associated with the electrochemical performance degradation is that there can be many electrical paths available across the electrochemical sites. Roughly speaking, electrical path consists of conduction parts and electrochemically activation sites. Potential loss associated with the former part is linear with current density, namely ohmic loss, while the potential loss in the latter part is not linear with current density, namely, non-ohmic loss. As a result, the followings are determined by this relation;

(1) Current path changes depending on total current density (Kawada et al. [62] for anode, Suzuki [63] for cathode).
(2) Higher oxide ion conduction in electrolyte leads to better electrode performance [64].
(3) In stack designs where the electrical path goes transversely though electrodes such as sealless tubular cells, the combination of ohmic resistance inside electrodes and electrolyte and electrode polarization resistance is essential in determining the current density distribution along the electrolyte [65].
(4) In stack designs where fuel and/or air flow is parallel to the electrolyte, the current density distribution largely depends on the location [66].

In view of these features, the degradation in electrochemical performance should be examined with careful investigations on the effect of current density. In what follows; the characteristic features in the cell level as well as the stack level will be described with an emphasis on those heats emitted during electrode reactions which depend largely on the current density.

2.4. Examples of cell level

The electrochemical reaction models are very important to correlate changes in chemical form or interdiffusion with cell performance degradation. One good example of indicating the importance of the overpotential on the degradation behaviour is the pioneer work by Taniguchi et al. [11,12] on the chromium poisoning; they made extensive investigations on chromium poisoning by changing the composition of cathodes, temperature and other factors and finally extracted the important conclusion that the life time (degradation rate) defined as the time for cell performance to become a half of the initial value is directly related with the observed overpotential expressed as $\log a(O) = \eta/2.303RT$, η and $a(O)$ being the overpotential of cathode and the activity of oxygen at the cathode/electrolyte interface, respectively. This relation strongly suggests that the driving force for the Cr poisoning is the oxygen potential gradient caused by the cathode overpotential. Usually, the overpotential increases with decreasing temperature so that their finding reasonably explains very interesting behaviour that the degradation due to the Cr poisoning is enhanced with decreasing temperature. This suggests that increasing temperature does not work as accelerating factors for the Cr poisoning.

Another good example indicating the relation between degradation and reaction models is the investigation on Cr poisoning by Matsuzaki and Yasuda who changed the combination of electrolyte and electrode among YSZ and SDC for electrolyte and LSM and LSCF for cathode [13]. This was interpreted in terms of the differences in the reaction mechanism, that is, the electrochemical active sites which are located in the vicinity of three phase boundary or over the cathode interfaces with the gas phase [20,21]. These differences can be originated from the conductivity of oxide ions, which are in turn determined by the oxide ion vacancy formation governed physicochemically by the valence stability of Mn^{4+}, Fe^{4+} and Co^{4+}. This enables us to understand the chemical stability of cathode and the Cr poisoning tolerance of cathode simultaneously by the same valence stability.

The effect of heats evolved will appear in the cell level as follows:

(1) In many cases, the degradation is detected by using electrochemical impedance spectroscopy (EIS). Here care must be exercised because in the EIS in the OCV vicinity, heat effects associated with the electrochemical reactions will not appear because both cathodic and anodic processes can be cancelled out the heat effect associated with the reversible electrochemical reaction.
(2) Heats evolved in the vicinity of the electrochemical active sites depends on current density. The Joule heats originated from the ohmic resistance of the electrolyte, the electrode, interconnects and other materials such as current collector are evolved inside such materials. When interface resistivity is large, a large amount of heats also evolve in the interface vicinity.
(3) Heats associated with both reversible and irreversible electrode reaction processes are evolved at the active sites. The non-linearity of the electrode polarization term against the current density tends to lead the concentration of current distribution. At the concentrated sites, the current density can become high and as a result, heats evolved can be enhanced, leading a kind of hot spots [67], depending on the thermal conductivity of associated materials, the operational temperature and so on.
(4) Effects of such local heating at the electrochemical sites are not so documented in literature. This is partly because of difficulty of measuring the local temperature distribution in the TPB vicinity, and partly because the SOFC electrodes

are good enough to be stable against such local heating. Even so, such local heating may affect significantly when electrodes are contaminated with impurities. For example, electrode behaviours in the presence of sulphur contaminant exhibit complicated features among literature. A clue to understand such complicated behaviour can be obtained from the considerations on local heating and associated with temperature changes in phase relation.

(5) For internal reforming reaction on anodes, the endothermic reforming reaction sites become cooler. This enhances vapour deposition reactions. An typical example is the SiO_2 deposition from the SiO(g) gas species at the reforming reaction cites which are close to the electrochemical reaction sites, leading a severe degradation of anodes.

2.5. Degradation of stacks/system

Heats evolved in stacks also depend on the current density. In a normal operation, the fuel utilization is kept at a high value such as 75–80%. When the current density increases, the heats evolved in the stacks also increase; this is partly because of the increasing amount of reactants and partly of lowering the efficiency of conversion to electricity. These evolved heats are used to heat up gases, leading to a steeper temperature distribution and further redistribution of current flow.

From the thermodynamic point of view, it is quite logical that heats evolve mainly at the electrochemical sites. Even so, this fact is not taken into account properly. Still, many modelling can work well to predict the behaviour of cells or stacks. This indicates that such local heating effect does not influence on cell performance when cells are operated in a normal manner. On the other hand, it is also recognized that degradation behaviours of SOFC full stacks are quite different from those of cells or short stacks. At present, there is no good explanation for this discrepancy. Here, considerations on local heating will provide a clue to understand such differences. Most important differences among cells, short stack and full stack are their heat management.

Another possible effect of increasing current density under the same utilization of fuel and air is that impurities in fuels or air which can be transported to electrochemical sites during a given period of time directly depend on the current density. If fuel is contaminated with sulphur, the effect of sulphur should depend on sulphur concentration as well as the current density under the same fuel utilization.

When stacks were damaged partly, degradation does not necessarily appear directly. This is particularly true for those damages in electrode activities. Since the current path will avoid such damaged parts, the degradation may appear as an increase in the ohmic resistance not as increase in the electrode polarization resistance. This makes it difficult to detect which parts are damaged from the impedance spectroscopy. In a stack level, this effect will be strengthened from the enhanced temperature distribution. Even though apparent degradation rate itself does not seem to be significant, severe damages can be taking place in a fatal manner. Inhomogeneous distribution of flows of gases, electrical path or temperature may enhance this tendency and therefore should be carefully avoided.

As summaries, the following is important:

(1) Electrode reaction models are important in correlating degradation with physicochemical properties.
(2) For cathodes, the valence stability of transition metal oxides is crucial, leading to different chemical stability/reactivity of the Sr component against the attack from acidic substances.
(3) For anodes, the soluble atoms in Ni should be carefully examined. Role of the oxide component should be also clarified.

2.6. Failure mode analysis

Since deterioration phenomena are closely related with each other, many changes can take place sequentially in a similar manner to chain reactions.

One of the examples is the effect of impurities involved in water to be used for reforming reaction [18]. Many impurities are decomposed or deposited at the entrance of the anode area, while gaseous species such as NaOH(g) or H_2S(g) go through the anode layers. Since Ni-based anodes are weak against H_2S(g), some degradation will take place. Outside anodes where remaining fuels will be combusted with air, such gaseous impurities lead to the formation of $NaSO_4$(l). This is the substance causing the hot corrosion for metal interconnects. Thus, impurities in water may cause different deteriorations among materials.

In this example, more serious phenomena can be involved; that is, liquid formation among the solid substances. Namely, the Ni–S eutectics and also the Na_2SO_4–NaCl–Na_2CrO_4 eutectics can be formed. Since sulphur contamination is frequently taking place in anode atmospheres, the formation of Ni–S eutectics or the dissolution of sulphur into nickel will lead to changes in microstructure, electrical path or electrode activity during thermal cycles or redox cycles. Furthermore, it is well known that the formation of Na_2SO_4-based eutectics causes hot corrosion [68]. In addition, there can be some possibility of affecting the nucleation of secondary phase formation or precipitation in ceramic substances such as cathode and other materials. For example, the $SrCrO_4$ formation is normally hindered from a (La, Sr)CrO_3 oxide interconnect plate although it is thermodynamically favoured and this precipitation reaction can take place in powers [69]. Similarly, the $SrCrO_4$ formation is thermodynamically predicted for the reaction of the (La, Sr)$FeO_{3-\delta}$ cathodes with chromium-containing gaseous species [20].

As summaries, failure mode analyses for entire stacks will be highly required. Effects of impurities in water to be utilized in reforming, air in addition to fuels should be clarified in more details.

2.7. Measuring degradation

Depending on the application, different approaches are followed to express the degradation of fuel cells. For tests that are close to the application (e.g. test of complete systems), the degradation is often expressed as relative degradation rates of power, voltage or efficiency. For test that are closer to fundamental research (e.g. single cell tests) it is often expressed as

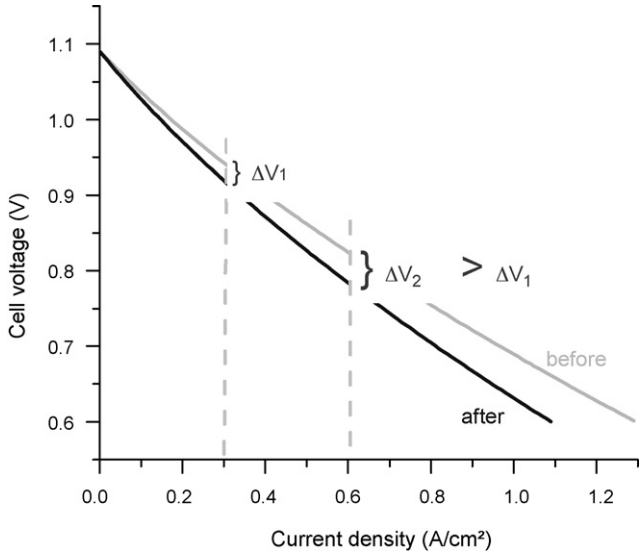

Fig. 2. *V–I* curves of an SOFC before and after long-term operation illustrating the mathematic–physical dependency of the voltage degradation from the operation conditions (i.e. current density). See also [70,41].

an increase of area specific resistances (ASRs), which were measured by electrochemical impedance spectroscopy.

When comparing the performance degradation at different operating conditions, one has to keep in mind that the operating conditions not only influence the degradation effects, but also influence the calculation of the degradation rates in a mathematical–physical way [70]. As illustrated in Fig. 2, the measured voltage degradation is obviously depending on the current density for a given ASR degradation. Assuming a linear *V–I* curve and a time-independent open circuit voltage, this effect results in a linear dependency of the voltage degradation rate from current density and ASR degradation rate:

$$\Delta V_{\mathrm{rel}}\,[\%] = \frac{I}{V_0}\,\Delta R_{\mathrm{abs}} = \frac{I}{V_0} R_0\,\Delta R_{\mathrm{rel}}\,[\%] \Rightarrow \Delta V_{\mathrm{rel}}\,[\%] \propto I \tag{4}$$

with ΔV: voltage degradation rate, I: electrical current, V_0: initial operating voltage, ΔR: resistance change

The additional dependency of ΔV [%] from V_0 increases this effect, as the operating voltage is lower at higher current densities. This has to be considered when judging the influence of the current densities on the degradation. The situation is even more complicated when other operating conditions are varied (e.g. temperature, gas composition) [70,71]. The best way to circumvent these problems is to record *V–I* curves and/or impedance spectra before and after the long-term operation at an identical operating point for all cells and then compare the ASR degradations.

3. Origin and mechanisms of anode degradation

The current state-of-the-art anode materials are Ni/YSZ and Ni/CGO cermets. They are fabricated as anode supports or thin films on the electrolyte using low cost techniques such as screen printing, tape casting or paint spraying, followed by a sintering process [72]. The fabrication of the microstructure and the final microstructural properties play a key role for the degradation of the Ni-anode under SOFC operating conditions.

Connected nickel–nickel particles serve as an electronic conductor. Furthermore nickel is the catalyst in the anode reaction. A ceramic network (YSZ or CGO) usually percolates around the nickel particles. The rigid ceramic structure adjusts the coefficient of thermal expansion (CTE) close to the electrolyte and inhibits the nickel from fast agglomeration during SOFC operation. Furthermore, it serves as a pathway for oxygen ion migration and therefore extends the triple phase boundary (TPB) into the anode. The TPB is the site where nickel, ceramic and pores meet and where the electrochemical reaction takes place. A porosity of 30–40 vol.% is necessary to supply the gas for the reaction and to remove the reaction products. Together, nickel, ceramic and pores form an interpenetrating network [73–76]. One model for the performance of SOFC electrodes which takes into account microstructural parameters was suggested by Costamagna et al. [77,78].

3.1. Microstructural changes

Under SOFC operating conditions the initial microstructure of the Ni-anode is changing. The most typical anode degradation phenomena, which can be observed after the experiment, are the agglomeration of nickel and loss of Ni–Ni contact [79–85], the change of nickel surface morphology, the break down of the ceramic network, the change in anode porosity, the separation of phases, horizontal and vertical cracking, delamination [86], coking [87], sulphur poisoning [88,89] and poisoning by other contaminants [90–93].

Figs. 3 and 4 show the microstructure of a Ni/ScSZ anode before and after the experiment in a five cells test rig, on 100 cm^2 round cells. The experiment was carried out at 950 °C in 4 g h^{-1} CPO-gas per cell. The initial electrical efficiency (DC) was approximately 30%. Two redox cycles of 14 h were simulated within 1000 h. Both pictures were taken on polished cross sec-

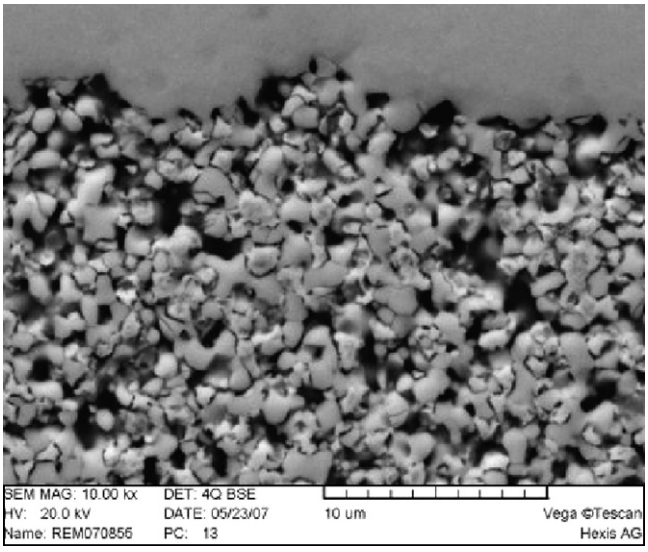

Fig. 3. Initial microstructure Ni/ScSZ anode after reduction.

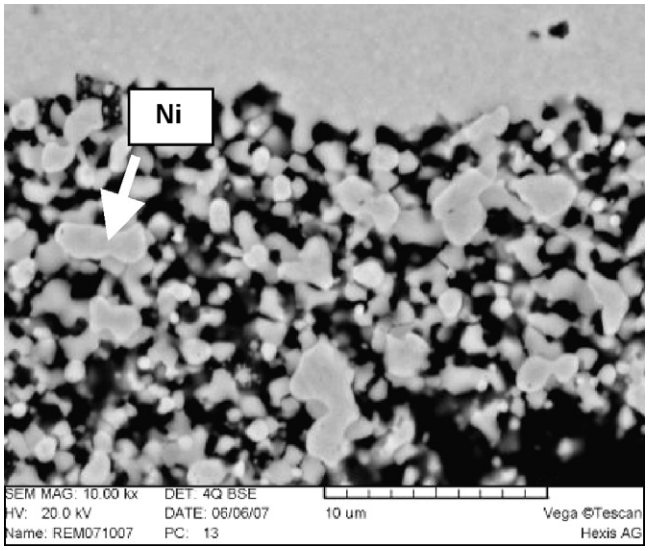

Fig. 4. Microstructure of the same Ni/ScSZ anode after the five cells stack experiment, 950 °C, CPO-gas, two redox cycles, 100 cm^2 cell.

tions, embedded in epoxy resin. After the experiment, the Ni–Ni contact is lost due to agglomeration to bigger particles. The porosity has increased and also the ScSZ-backbone seems to be damaged.

It is widely accepted that the degradation of the anode microstructure results in a decrease of the overall cell performance and a corresponding increase of the area specific resistance on long term [73,74,79,80,94,95]. The cell resistance can be measured in situ by electrical impedance spectroscopy. Impedance spectra give information on ohmic- and polarization losses. This is very useful to investigate certain rate limiting steps and their changes over time. By observing the increase in the ohmic and/or polarization resistances under controlled SOFC operating conditions, certain degradation phenomena can be identified [79,80,94,96]. In general, an increase of the ohmic loss correlates with the conductivity of the cell components [97], interfacial reactions and the contacting resistance [98,99]. In contrast, the polarisation resistance depends on the number of electro-catalytic active sites, the gas composition, and the concentration of gases near the triple phase boundary. Single processes of the polarisation loss appear in characteristic frequency domains and can therefore be identified by varying the operating conditions (e.g. temperature or gas composition). However, detailed knowledge about the cell under operating conditions is needed to extract the anode losses from the overall loss of the cell [66,96,100–104].

It should be noted that the ohmic- and polarisation resistances can also be influenced by cell design, stack and system parameters. Especially, for the anode the interplay between contacting and in-plane conductivity becomes important in real stack experiments. On larger cells, e.g. of 100 cm^2, the contacting is hardly perfect and the contacting area usually not more than 50%. Therefore, the migration path for electrons increase from micrometres under the neps, to millimetres under the channels, leading to current/potential distributions which will locally impact the ohmic and the polarisation resistances [98,99,105].

3.2. Anode degradation mechanisms

Microstructural changes result from different degradation mechanism. For the Ni cermet anode, three major mechanisms should be distinguished: (1) material transport mechanisms, (2) deactivation and passivation mechanisms and (3) thermomechanical mechanisms.

Each of those mechanisms may become dominant under certain operating conditions such as the steady state mode, the redox- or thermocycling mode, or in case of other stack and system failures. Under real operating conditions, an interaction of those degradation mechanisms can be observed.

Two important *material transport* phenomena are (1) the change in Ni surface morphology and (2) the increase in Ni particle size. Both processes are mainly driven by the affinity of nickel to reduce its free surface energy under SOFC operating conditions. Nickel atoms are transported by evaporation/condensation- and diffusion mechanisms. Those mechanisms are highly dependent on the operating conditions especially temperature and water vapour content. The growth of a big particle on the costs of a small particle is known as Ostwald ripening [106]. The decrease of the specific surface area correlates with the number of catalytic active sites and therefore the polarisation resistance increases [79]. On the other hand, Ni agglomeration leads to a disconnection of Ni–Ni particles and therefore the conductivity decreases [107].

The degradation of SOFC anodes due to sintering of metal particles was modelled by Ioselevich et al. [6] and Abel et al. [108]. Furthermore, the sintering of Ni was investigated and modelled for other technologies e.g. nickel steam reforming [109–112].

The decrease of the chemical potential is another driving force for material transport mechanisms in the Ni anode. Chemical gradients can result from impurities and improper material combinations [90–93].

Sulphur poisoning [88,89], coking [87] and poisoning by other impurities [90–93] are known *deactivation mechanisms* for the nickel anode. The active sites and/or the pore network get blocked and lead to an increase mainly of the polarisation resistance.

Thermomechanical mechanisms arise from residual stresses and lead to a delamination or a cracking of the anode. They are influenced by the interplay of material-, stack- and system parameters and generally increase with increasing cell size [113–116].

3.3. Operating conditions

The kinetics of most of the anode degradation mechanisms is influenced by the operating conditions of the SOFC. Two cases of operating conditions should be distinguished: (1) the steady state mode and (2) the transient mode. The steady state mode shows a time related degradation which often occurs in three phases. The first phase is often ascribed to the reorganisation of the electrode microstructures which can lead to an increase or decrease of the performance. The second phase

shows a continuous degradation rate whereas the performance decreases rapidly in the third phase. The transient mode which is in practice a redox or a thermal cycle shows an accelerated degradation and sometimes a rapid decease of the performance occurs [86].

The most important operating parameters for the anode degradation in the steady state mode are temperature [80,82,96], gas composition, especially the partial pressure of water [95,96] and the current density, in other words, the working potential [94]. In terms of anode degradation, a strong interaction between those parameters has been indicated.

Thermodynamic calculations and experiments show that there is a potential where the Ni starts to be oxidized to NiO at a certain temperature [94].

In contrast, the number of redox and thermal cycles is the most critical parameter of the transient mode [16,83,84, 107,117–127]. Practically, those cycles occur due to system failures e.g. in electronic devices. Especially, the redox stability of state-of-the-art Ni anodes is one of the major drawbacks. The change in particle size from Ni to NiO and back to Ni leads to irreversible changes in the microstructure [16,83,117,119].

For electrolyte supported cells, accelerated coarsening of the nickel particles has been observed after several redox cycles leading to an accelerated decrease of the cell performance [83,86].

In contrast, cracking of the electrolyte is the major drawback for the anode supported cell under redox cycling conditions [16,107,118]. Irreversible volume expansion has been measured on anode substrates and pellets in the dilatometry test rig after each redox cycle [119]. Cracks in the electrolyte significantly lower the OCV and lead to a breakdown of the cell voltage in the worst case.

3.4. Outlook

In the last years huge progress has been made in the understanding of the interplay between processing, performance, working conditions and the degradation of the Ni cermet materials. However, a remaining challenge is the improvement of anode integration into stack- and system concepts. It is believed that many thermomechanical and deactivation mechanisms can be solved by improved stack designs and concepts, system solutions, and improved quality control. In contrast, material solutions to inhibit Ni-transport, enhance redox stability and sulphur tolerance are still critical. With respect to that, it is still questionable how a microstructure has to be designed to match the required lifetime of >40,000 h. Novel materials being tolerant against redox cycles [128] and sulphur contaminants [129] show first promising results. However, they will most likely not be ready in short-term.

4. Cathode degradation mechanisms

4.1. Potential degradation mechanisms

Cell performance degradation related to the SOFC cathode is mostly caused by the following effects:

(1) coarsening of the microstructure due to sintering;
(2) decomposition of the cathode material;
(3) chemical reaction with electrolyte to form insulating phases at interfaces;
(4) spallation of the cathode;
(5) poisoning of the cathode (e.g. by chromium species).

As a result of these effects, the electronic or ionic conductivity, as well as the electro-catalytic activity of the cathode material, the electrochemically active surface area, or the porosity will decrease, which then results in a decreased performance of the cell. All of these effects are dependant on each other and may be influenced by the operating parameters (e.g. operating temperature, current density, overvoltage, oxygen and water partial pressures (humidity) in air) of the cell. To find out about the degradation origins, it is helpful to look at the influence of operating parameters on the degradation. This may also help to find "safe" operating conditions.

The effects described in the literature are different for the various state-of-the-art cathode materials. This paper describes some of the effects that have been found for lanthanum manganites (e.g. LSM) and lanthanum iron–cobaltites (LSCF, LSF). The focus was set on "intrinsic" degradation mechanisms, although "extrinsic" degradation effects, like chromium poisoning of the cathodes, are dominant for most of the real SOFC systems that include metallic interconnects.

4.2. Degradation of manganese-based cathodes (e.g. LSM)

Manganese-based perovskites can be regarded as being the most common SOFC cathode materials. They are most commonly used with lanthanum and strontium or calcium on the A-site with Sr, Ca contents of 10–40% and a small (5%) A-site deficiency: e.g. $La_{0.65}Sr_{0.3}MnO_{3\pm\delta}$ or $La_{0.8}Sr_{0.15}MnO_{3\pm\delta}$ (LSM). For best performance, these materials are mixed with ionic conductors (e.g. yttria stabilized zirconia, YSZ) as composite cathodes.

One potential degradation mechanism is the chemical reaction of LSM with YSZ to form insulating phases like $SrZrO_3$ or La_2ZrO_7 [8,130]. This can already occur during sintering of the cathodes at high temperatures. Minh and Takahashi [1] have summarized the potential reaction products of LSM and YSZ depending on the Sr content and the temperature. From their figure, a Sr content of 30% can be considered as optimal against the formation of unwanted phases. The reactivity can be further decreased by using materials with a small A-site deficiency. According to calculations of [27,53], this is not sufficient to prevent La_2Zr_2O7 formation for the Sr-less $LaMnO_{3\pm\delta}$–YSZ system [27,53], although still it may be sufficient for $La_{1-x-y}Sr_xMnO_{3\pm\delta}$ ($x \geq 0.2$)–YSZ [28]. For a more comprehensive review on the compatibility between LSM and YSZ see [8].

To prove the compatibility of LSM and YSZ with commercially available powders, 8YSZ (Tosoh, Japan) and LSM (H.C. Starck, Germany) have been mixed in ethanol, were pressed to pellets and exposed to heat. After the heat exposure, the pellets were crushed in a mortar. The phase composition of the result-

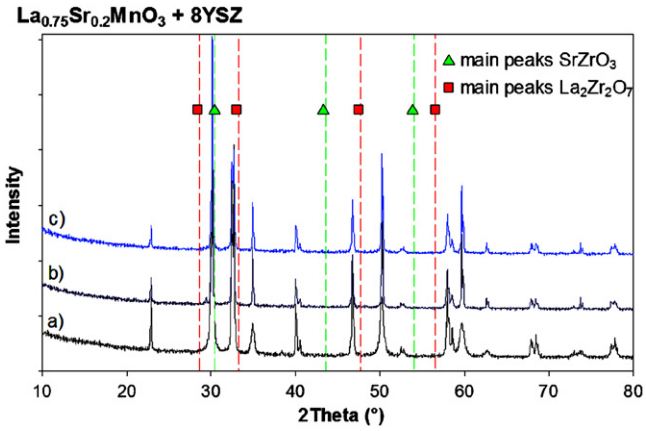

Fig. 5. X-ray diffractograms of 50% $La_{0.75}Sr_{0.2}MnO_{3\pm\delta}$ + 50% 8YSZ powder mixtures (a) without heat treatment, (b) after 24 h exposure to 1200 °C and (c) after 990 h exposure to 1400 °C. The potential peak positions of the undetected phases $SrZrO_3$ and $La_2Zr_2O_7$ are also shown.

ing powder was analysed by XRD at EMPA, Dübendorf with a Panalytics PW 3040 with Cu K_α radiation (see Fig. 5). The analysis of the powder mixtures did not show any reactive phases even after prolonged exposition of the powder pellets to temperatures exceeding the usual sintering and operating temperatures, at least within the limit of detection limit of this technique (about 2%).

Even if these unwanted reactions do not occur during simple high temperature heat treatment of the mixtures, i.e. in non-operating conditions, they may still take place during operation of the fuel cell. Heneka and Ivers-Tiffée [131] have seen a strong performance degradation after several hundred current cycles with overpotentials higher than 400 mV. The degradation was found to be the result of La_2ZrO_7 formation followed by spallation of the cathode. New results from the same group [132] show, that not the cycling, but the high overpotential is the initial reason for the zirconate formation. In agreement with these findings, Hagen et al. [133] have seen a strong increase of the voltage degradation when operating the cells at high current densities (>0.5 A cm^{-2}) and low temperatures (750 °C), i.e. at overpotentials higher than 300 mV. This was probably also the result of zirconate formation reaction which becomes favoured at the reducing atmospheres (higher overpotentials) as predicted from the thermodynamic considerations [8].

Also, manganese diffusion from LSM into the YSZ electrolyte has been observed [131]. This can lead to a decrease of the ionic and an increase of the electronic conductivity of the electrolyte section close to the cathode [134,135]. While mainly occurring during sintering, this effect is generally not considered as a major degradation mechanism during SOFC operation.

To our knowledge, coarsening of the LSM/YSZ cathode has not yet been reported as being a significant cell degradation mechanism although this may occur at high operating temperatures (>900 °C) particularly for the A-site deficient LSM. A coarsening and blocking effect has however been reported due to the influence of chromium, copper and cobalt, which partly form spinel phases with the manganese of the cathode.

Despite the possible degradation mechanisms, many groups have operated SOFCs with manganese-based cathodes for several thousand hours. In all cases where they were operated without chromium-containing metallic interconnectors, low degradation rates below 1% could be realized [136,137], while Siemens has demonstrated more than 70,000 h of operation with tubular cells based on lanthanum manganese cathodes without significant degradation [138]. Consequently, the intrinsic degradation of manganese-based cathodes seems to be of minor importance for the long-term stability of SOFCs as long as certain operating conditions, like high overpotentials and very low oxygen partial pressures on the cathode side are avoided.

4.3. Degradation of ferro-cobaltite cathodes (e.g. LSCF)

Cells with LSCF-based cathodes were measured to have a significantly higher performance than cells with LSM/YSZ cathodes [71,139], but the degradation rates for SOFCs with LSCF (e.g. $La_{0.58}Sr_{0.4}Co_{0.2}Fe_{0.8}O_{3-\delta}$) cathodes were also found to be slightly higher than for cells with LSM/YSZ-based cathodes [70,71,137].

In contrast to the manganese-based cathodes, LSCF and YSZ react to unwanted phases like $SrZrO_3$ already when exposed to 1210 °C or even 700 °C for several hundred hours [71]. This can also occur despite a CGO interlayer, as Sr may diffuse through the interlayer, especially during sintering [71,137,140].

As described in [71,141] the influence of the operating parameters was investigated. For this, the ASRs of the cells were determined before and after the long-term testing by electrical impedance spectroscopy at 700 °C. Fig. 6 shows the relative ASR change depending on the three parameters, namely, temperature, current density and oxygen content on the air side of the cell. The degradation was dominated by an increase of the polarisation resistance and a small increase of the ohmic resistance. The degradation at 800 °C was significantly higher than at 700 °C, while a decreased oxygen content (5% instead of 21% O_2) resulted in a slightly lower degradation. The current

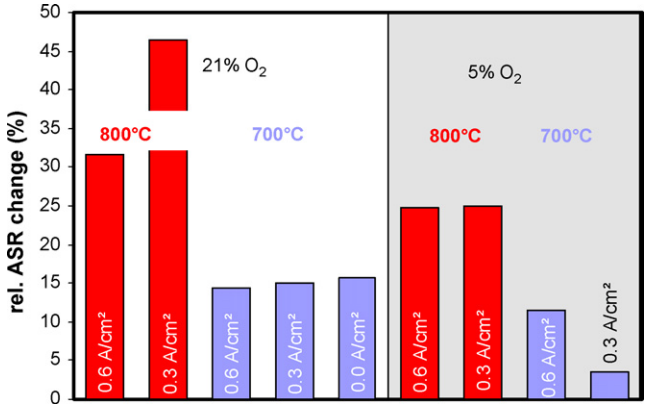

Fig. 6. Relative change of the area specific resistance (ASR) due to approximately 1000 h operation at the given operation conditions (temperature, current density, oxygen content). The ASR values were determined by impedance spectroscopy before and after the long-term operation. Measurement conditions chosen identically for all cells: 700 °C, OCV, gases: 250 min^{-1} H_2 + 5% H_2O and air, active area: 1 cm^2. Data from [141].

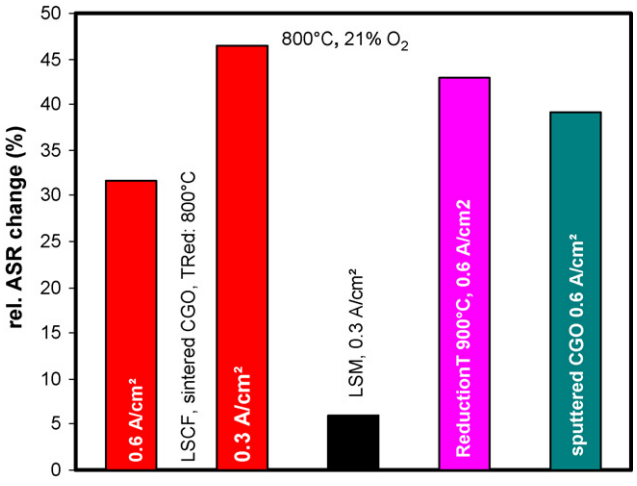

Fig. 7. Relative change of the area specific resistance (ASR) due to approximately 1000 h operation of cells with modifications (LSM/YSZ cathode, 900 °C reduction temperature, sputtered CGO interlayer) in comparison to the left-most reference cells. The ASR values were determined by impedance spectroscopy before and after the long-term operation. Measurement conditions chosen identically for all cells: 700 °C, OCV, gases: 250 ml min^{-1} H_2 + 5% H_2O and air, active area: 1 cm^2. Data from [141].

density had no clear effect on the degradation. If we additionally consider, that the voltage–time curve of the left-most cell (0.6 A cm^{-2}, 800 °C, 21% O_2) was different than for all the other cells [141], it seems that the current density did not influence the cell degradation significantly.

Similarly to these cells, some modified cells were tested (see Fig. 7); one with an anode that was reduced at 900 °C instead of 800 °C. This was meant to decrease the coarsening of the anode microstructure during operation, as the microstructure at the beginning was supposed to be coarser after reducing at higher temperatures. No significant influence for the ASR degradation could be found. Another cell was manufactured with a nearly dense, sputtered CGO interlayer (as described in [142]), to prevent Sr-diffusion through the interlayer. This slightly lowered the total ASR degradation and significantly lowered the degradation of the ohmic resistance. Apparently, the $SrZrO_3$ formation was successfully suppressed by this measure, but the main degradation mechanism was not suppressed, as the increase of the polarization resistance was the same. A third cell with an LSM/YSZ cathode was also measured. This cell showed hardly any degradation within the 1000 h, but a significant decrease of the ohmic resistance [141] in the first 500 h, which might be a result of an increase in the electronic conductivity of the cathode due to sintering of the rather coarse current collection layer that was used. Similar effects are described in the literature as "electrode activation" [143,144], but are mostly described as influencing the polarization resistance. The increase of the polarization resistance within 1000 h was much smaller than for the LSCF-based cells.

The measurements have given clear indications that the causes of the degradation are to be found in the properties influencing the electrochemical performance of LSCF. While no obvious coarsening of the microstructure could be determined for these cells [145], another change of the cathodes was visible to the naked eye: after the measurements, the cathodes were surrounded by a grey-brownish rim, which was more pronounced on the gas outlet side of the cathode [146] and more intense after operation at 800 °C than at 700 °C. While no reason for this could be found by EDX/SEM-analyses, SIMS measurements revealed that strontium and to less extent lanthanum had been diffusing out of the cathode on the grain surfaces of the underlying CGO interlayer. The diffusion of strontium out of the cathode leads to a strontium depletion of the LSCF cathode, which is supposed to significantly lower the performance of the LSCF and to be the major degradation mechanism for these cells. Measurements on cells with slightly less strontium in the cathode ($La_{0.58}Sr_{0.38}Co_{0.2}Fe_{0.8}O_{3-\delta}$) showed lower performance than the $La_{0.58}Sr_{0.4}Co_{0.2}Fe_{0.8}O_{3-\delta}$ [145].

Sr segregation is also seen as the main degradation mechanism for LSCF by Simner et al. [137], who have detected Sr enrichment by XPS close to the cathode and on its surface after operation. They have also discussed the possible segregation mechanisms in more detail.

More recently, measurements on cells with cathode materials having Pr instead of La on the A-site, that is, $Pr_{0.58}Sr_{0.4}Co_{0.2}Fe_{0.8}O_{3-\delta}$, showed slightly lower degradation rates than the corresponding LSCF cathodes, pointing to an increased stability of these perovskites [147]. The measurements were however considered not long enough for a definite statement on this.

With respect to chromium poisoning, mixed electronic-ionic conducting cathodes, like LSCF are probably more resistant than LSM/YSZ cathodes, because the electrochemically active area is not restricted to the triple phase boundary. This was confirmed by measurements from [13] and [148], while [149] have seen a similar degradation. It is agreed, that the mechanisms are different for the different cathodes [20,148–150]: For LSM/YSZ, chromium condenses close to the electrolyte, partly forming $(Mn, Cr)_3O_4$ spinel phases, while chromium and LSCF seem to form $SrCrO_4$ mainly at the cathode surface. Which of these effects is worse in the long-run is still under evaluation. The chromium poisoning effects are likely to be influenced by the overpotential on the cathode side and therefore the current density, which has to be considered when studying these effects.

4.4. Degradation of other cathode materials

The pure ferrites (La, Sr)$FeO_{3\pm\delta}$ (LSF) are thermodynamically more stable than the cobalt-containing perovskites [21]. However, it was measured that they were also less performing than LSCF with a similar A-site stoichiometry [139,151]. A potential degradation mechanism for LSF cathodes is the interdiffusion of Zr and La as described by [152,153]. Therefore, a barrier layer (e.g. doped ceria) is also necessary. To our knowledge, other effects of intrinsic degradation of LSF cathodes in complete cells have not yet been published, although a significant degradation over 500 h has been reported when LSF is contacted with an inert material like gold [154].

Recently, several groups have worked on cathode materials with a K_2NiF_4-structure (e.g. $La_2NiO_{4+\delta}$, $Nd_2NiO_{4+\delta}$, $La_2(Fe,$

Ni)$O_{4+\delta}$). Lalanne et al. [155] have shown voltage degradation rates of 5% per 1000 h over 800 h of operation, but that was probably mainly a result of non-cathode related degradation effects. Orui et al. [156] have operated cells with $LaNi_{0.6}Fe_{0.4}O_{3\pm\delta}$ for about 1400 h, observing only an activation of the cells due to the elimination of unwanted reaction phases between LNF and YSZ during operation. This reduction of the cathode resistance was larger than any potential degradation effect. To our knowledge, no evidences for an intrinsic degradation, but also no other long-term (>500 h) experiments for cells with these cathodes have been published, yet.

5. Summaries

It is widely accepted that changes in the state-of-the-art Ni-cermet anode microstructure result in a decrease of the cell performance in the long term. The microstructural changes in the anode are seen as a drawback to achieve the required cell lifetime of >40,000 h. It is assumed, that all major anode degradation mechanisms are known. In contrast, material solutions to achieve redox stability, sulphur tolerance and to inhibit nickel agglomeration at the same time are still missing. Therefore, one approach to reduce the microstructural degradation of the Ni cermet anode is to avoid unfavourable operating conditions and to tailor the anode to the specific stack and system designs.

On the cathode side, several materials are common, which also implies several degradation mechanisms. The manganese-based cathodes (LSM) have been tested to be sufficiently stable for more than 70 000 h as long as critical operating conditions (e.g. high overvoltages) and poisoning (e.g. by chromium vapours) are avoided. Cathode materials with better performance at low temperatures (<750 °C), like doped lanthanum ferro-cobaltites have shown less stability and intrinsic degradation, which is probably mainly due to a decomposition of the perovskite. Although the resulting degradation rates will probably not play a major role in most complete systems today, work on more stable and still high-performing cathode materials has to be continued.

For both anodes and cathodes, it is highly hoped that understanding the degradation mechanisms should be deepened to obtain correlations with materials fundamental properties and electrode reaction mechanisms and to make it possible to establish the durability and reliability of the SOFC stacks/systems.

Acknowledgements

The research on the material properties of the degraded LSCF cathodes was made at Forschungszentrum Jülich (IEF-1). A. Mai likes to thank his former colleagues at Forschungszentrum Jülich for their involvement in that work, especially F. Tietz and also U. Breuer for the SIMS measurements, as well as M. Becker (University Karlsruhe).

B. Iwanschitz likes to thank the Swiss Office of Energy (BfE) and the swiss*electric* research funding for the financial support within the frame of the swiss SOF-CH project.

References

[1] N.Q. Minh, T. Takahashi, Science and Technology of Ceramic Fuel Cells, Elsevier, Amsterdam, 1995.
[2] H. Yokokawa, N. Sakai, in: W. Vielstich, A. Lamm, H.A. Gasteiger (Eds.), Handbook of Fuel Cells Fundamentals Technology and Application, vol. 1, John Wiley & Sons, 2003, pp. 219–266.
[3] S.C. Singhal, Solid Oxide Fuel Cells VI, PV 99-19, The Electrochemical Society, Inc., Pennington, NJ, USA, 1999, pp. 39–51.
[4] A.C. Müller, A. Weber, D. Herbstritt, E. Ivers-Tiffee, in: S.C. Singhal, M. Dokiya (Eds.), Proceedings of the Eighth International Symposium on Solid Oxide Fuel Cells (SOFC-VIII), PV 2003-07, The Electrochemical Society, Pennington, NJ, 2003, pp. 196–199.
[5] D. Skarmoutsos, F. Tietz, P. Nikolopoulos, Fuel Cells 1 (2001) 243–248.
[6] A. Ioselevich, A.A. Kornyshev, W. Lehnert, Solid State Ionics 124 (1999) 221–237.
[7] T. Matsui, T. Iida, M. Kawano, T. Inagaki, R. Kikuchia, K. Eguchi, in: K. Eguchi, S.C. Singhal, H. Yokokawa, J. Mizusaki (Eds.), Proceedings of the Tenth International Symposium on Solid Oxide Fuel Cells (SOFC-X), The Electrochemical Society, Pennington, NJ, ECS Trans. 7 (1) (2007) 1437–1445.
[8] H. Yokokawa, Annu. Rev. Mater. Res. 33 (2003) 581–610.
[9] S.P. Simner, M.D. Anderson, M.H. Engelhard, J.W. Stevenson, Electrochem. Solid-State Lett. 9 (10) (2006) A478–A481.
[10] S.P. Jiang, ZhangF S., Y.D. Zhen, J. Electrochem. Soc. 153 (2006) A127–A134.
[11] S. Taniguchi, M. Kadowaki, H. Kawamura, T. Yasuo, Y. Akiyama, Y. Miyake, T. Saitoh, J. Power Sources 55 (1995) 73–79.
[12] S. Taniguchi, M. Kadowaki, T. Yasuo, Y. Akiyama, Y. Itoh, Y. Miyake, K. Nishio, Denki Kagaku 64 (6) (1996) 568–574.
[13] Y. Matsuzaki, I. Yasuda, Solid State Ionics 132 (2000) 271–278; Y. Matsuzaki, I. Yasuda, J. Electrochem. Soc. 148 (2001) A126.
[14] P. Batfalsky, V.A.C. Haanappel, J. Malzbender, N.H. Menzler, V. Shemet, I.C. Vinke, R.W. Steinberger, J. Power Sources 155 (2006) 128–137.
[15] D. Sarantaridis, A. Atkinson, Fuel Cells 7 (2007) 246–258.
[16] D. Waldbillig, A. Wood, D.G. Ivey, J. Power Sources 145 (2005) 206–215.
[17] W. Bujalski, C.M. Dikwal, K. Kendall, J. Power Sources 171 (2007) 96–100.
[18] H. Yokokawa, T. Watanabe, A. Ueno, K. Hoshino, ECS Trans. 7 (2007) 133–140.
[19] H. Yokokawa, T. Horita, N. Sakai, T. Kawada, M. Dokiya, Solid State Ionics 78 (1995) 203–210.
[20] H. Yokokawa, T. Horita, N. Sakai, J. Yamaji, M.E. Brito, Y.P. Xiong, H. Kishimoto, Solid State Ionics 177 (2006) 3193–3198.
[21] H. Yokokawa, H. Sakai, T. Horita, K. Yamaji, M.E. Brito, H. Kishimoto, J. Alloy Compd. 452 (2008) 41–47.
[22] K. Hilpert, J. Electrochem. Soc. 136 (7) (1989) 2099–2108.
[23] H. Flood, T. Førland, Acta Chem. Scand. 1 (1947) 592.
[24] J. Maier, Chem. Eur. J. 7 (2001) 4762–4770.
[25] S. Yamaguchi, K. Nakamura, T. Higuchi, S. Shin, Y. Iguchi, Solid State Ionics 136–137 (2000) 191–195.
[26] H. Yokokawa, N. Sakai, T. Kawada, M. Dokiya, Denki Kagaku 57 (1989) 821 (in Japanese).
[27] H. Yokokawa, N. Sakai, T. Kawada, M. Dokiya, Denki Kagaku 57 (1989) 829 (in Japanese).
[28] H. Yokokawa, N. Sakai, T. Kawada, M. Dokiya, Denki Kagaku 58 (1990) 161 (in Japanese).
[29] H. Yokokawa, N. Sakai, T. Kawada, M. Dokiya, J. Am. Ceram. Soc. 73 (1990) 649.
[30] H. Yokokawa, N. Sakai, T. Kawada, M. Dokiya, Solid State Ionics 40/41 (1990) 398.
[31] H. Yokokawa, N. Sakai, T. Kawada, M. Dokiya, Denki Kagaku 58 (1990) 489.
[32] H. Yokokawa, N. Sakai, T. Kawada, M. Dokiya, J. Electrochem. Soc. 138 (1991) 1018.
[33] H. Yokokawa, N. Sakai, T. Kawada, M. Dokiya, J. Electrochem. Soc. 138 (1991) 2719.

[34] H. Yokokawa, N. Sakai, T. Kawada, M. Dokiya, Solid State Ionics 52 (1992) 43.
[35] H. Yokokawa, T. Horita, N. Sakai, M. Dokiya, Solid State Ionics 86–88 (1996) 1161–1165.
[36] H. Yokokawa, N. Sakai, T. Kawada, M. Dokiya, Science and Technology of Zirconia V, Technomic Publishing Comp, Lancaster, Pennsylvania, 1993, pp. 59–68.
[37] H. Yokokawa, N. Sakai, T. Horita, K. Yamaji, Y.-P. Xiong, T. Otake, H. Yugami, T. Kawada, J. Mizusaki, J. Phase Equilib. 22 (3) (2001) 331–338.
[38] H. Yokokawa, T. Kawada, M. Dokiya, J. Am. Ceram. Soc. 72 (1989) 152.
[39] H. Yokokawa, N. Sakai, T. Kawada, M. Dokiya, J. Solid State Chem. 94 (1991) 106.
[40] H. Yokokawa, T. Kawada, M. Dokiya, J. Am. Ceram. Soc. 72 (1989) 2104.
[41] H. Yokokawa, J. Phase Equilib. 20 (3) (1999) 258–287.
[42] H. Yokokawa, K. Yamaji, T. Horita, N. Sakai, CALPHAD 24 (4) (2001) 435–448.
[43] H. Yokokawa, S. Yamauchi, T. Matsumoto, CALPHAD 26(2), (2002) 155–166, see also the following website: http://www.kagaku.com/malt/index.html.
[44] L. Kaufman, H. Bernstein, Computer Calculation of Phase Diagrams, Academic Press, New York and London, 1970.
[45] L.H. Bennett (Ed.), Computer Modelling of Phase Diagrams, TMS, Warrendale, PE, 1986.
[46] J.-O. Anderson, T. Helander, L. Hoeglund, P. Shi, B. Sundman, CALPHAD 26 (2) (2002) 273–312, see also the following web site http://www.thermocalc.com/index.html.
[47] A. Nicholas Grundy, B. Hallstedt, L.J. Gauckler, J. Phase Equilib. 24 (1) (2003) 21–37.
[48] M. Chen, B. Hallstedt, L.J. Gauckler, J. Phase Equilib. 24 (3) (2003) 212–227.
[49] A. Nicholas Grundy, B. Hallstedt, L.J. Gauckler, Acta Mater. 50 (2002) 2209–2222.
[50] A. Nicholas Grundy, M. Chen, B. Hallstedt, L.J. Gauckler, J. Phase Equilib. 26 (2) (2005) 131–151.
[51] A. Nicholas Grundy, B. Hallstedt, L.J. Gauckler, CALPHAD 28 (2004) 191–201.
[52] M. Chen, B. Hallstedt, L.J. Gauckler, Solid State Ionics 176 (2005) 1457–1464.
[53] M. Chen, A. Nicholas Grundy, B. Hallstedt, L.J. Gauckler, CALPHAD 30 (4) (2006) 489–500.
[54] M. Chen, B. Hallstedt, L.J. Gauckler, CALPHAD 29 (2005) 103–113.
[55] S.K. Lau, S.C. Singhal, Proc. Corros. 85 (1985) 79.
[56] J. Echigoya, S. Hiratsuka, H. Suto, Mater. Trans. JIM 30 (1989) 789.
[57] A.N. Kornilov, I.M. Ushakova, S.M. Skuratov, Russ. J. Phys. Chem. 41 (1967) 101.
[58] M. Bolech, E.H.P. Cordfunke, F.J.J.G. Janssen, A. Navrotsky, J. Am. Ceram. Soc. 78 (1995) 2257.
[59] K. Hilpert, in: M.J. Clarke, J.B. Goodenough, J.A. Ibers, C.K. Jorgensen, D.M.P. Mingos, J.B. Neilands, G.A. Palmer, D. Reinen, P.J. Sadler, R. Weiss, R.J.P. Williams (Eds.), Structure and Bonding, Noble gas and High Temperature Chemistry, vol. 73, Springer, Berlin, 1990, pp. 97–198.
[60] V.L. Stolyarova, G.A. Semenov, Mass Spectrometric Study of the Vaporization of Oxide Systems, John Wiley & Sons, Chichester, 1994.
[61] N.S. Jacobson, E.J. Opila, D.L. Myers, E.H. Copland, J. Chem. Thermodyn. 37 (2005) 1130–1137.
[62] T. Kawada, N. Sakai, H. Yokokawa, M. Dokiya, M. Mori, T. Iwata, J. Electrochem. Soc. 137 (1990) 3042.
[63] M. Suzuki, et al., In Proceedings of the 2nd IFCC (International Fuel Cell Conference), Kobe, NEDO, 1966.
[64] H. Uchida, M. Yoshida, M. Watanabe, J. Electrochem. Soc. 146 (1) (1999) 1–7.
[65] D.C. Fee, S.A. Zwick, J.P. Ackerman, Proceedings Conference on High Temperature Solid Oxide Electrolytes, vol. 1, Anion Conductors, Brookhaven National Laboratory, 1983, pp. 29–38 (compiled by F.J. Salzano).
[66] S. Primdahl, M. Mogensen, J. Electrochem. Soc. 145 (7) (1998) 2431–2438.
[67] T. Kawada, T. Horita, N. Sakai, H. Yokokawa, M. Dokiya, J. Mizusaki, Solid State Ionics 131 (2000) 199–210.
[68] N. Otsuka, R.A. Rapp, J. Electrochem. Soc. 137 (1990) 53–60.
[69] S. Miyoshi, S. Onuma, A. Kaimai, H. Matsumoto, K. Yashiro, T. Kawada, J. Mizusaki, H. Yokokawa, J. Solid State Chem. 177 (2004) 4112–4118.
[70] M. Becker, A. Mai, E. Ivers-Tiffée, F. Tietz, in: S.C. Singhal, J. Mizusaki (Eds.), Solid Oxide Fuel Cells IX (SOFC-IX), The Electrochemical Society, Pennington, USA, 2005, p. 514.
[71] A. Mai, M. Becker, W. Assenmacher, F. Tietz, D. Hathiramani, E. Ivers-Tiffée, D. Stöver, W. Mader, Solid State Ionics 177 (2006) 1965–1968.
[72] C. Voisard, U. Weissen, E. Batawi, R. Kruschwitz, 5th European Solid Oxide Fuel Cell Forum, Lucern, 2002, pp. 18–25.
[73] T. Fukui, S. Ohara, M. Naito, K. Nogi, J. Eur. Ceram. Soc. 23 (2003) 2963–2967.
[74] J.H. Lee, J.W. Heo, D.S. Lee, J. Kim, G.H. Kim, H.W. Lee, H.S. Song, J.H. Moon, Solid State Ionics 158 (2003) 225–232.
[75] H. Tu, U. Stimming, J. Power Sources 127 (2004) 284–293.
[76] W.C. Zhu, S.C. Deevi, Mater. Sci. Eng. A362 (2003) 228–239.
[77] P. Costamagna, P. Costa, V. Antonucci, Electrochim. Acta 43 (3–4) (1998) 375–394.
[78] P. Costamagna, M. Panizza, G. Cerisola, A. Barbucci, Electrochim. Acta 47 (2002) 1079–1089.
[79] K. Norgaard Toft, D. Lybye, M. Mogensen, C. Hatchwell, Solid State Electrochemistry, Proceedings of the 26th Risø International Symposium, 2005.
[80] A. Hagen, R. Barfod, P.V. Hendriksen, Y.L. Liu, S. Ramousse, J. Electrochem. Soc. 153 (6) (2006) A1165–A1171.
[81] D. Simwonis, F. Tietz, D. Stöver, Solid State Ionics 132 (2000) 241–251.
[82] T. Iwata, J. Electrochem. Soc. 143 (5) (1996) 1521–1525.
[83] E. Batawi, C. Voisard, U. Weissen, J. Hoffmann, Y. Sikora, J. Frei, 6th European Solid Oxide Fuel Cell Forum, Lucerne, 2004, pp. 767–773.
[84] D. Fouquet, A.C. Müller, A. Weber, E. Ivers-Tiffée, 5th European Solid Oxide Fuel Cell Forum, Lucerne, 2002, pp. 467–474.
[85] D. Simwonis, ISSN 0944-2952 Thesis, University Bochum, 1999.
[86] B. Iwanschitz, J. Sfeir, A. Mai, T. Hocker, International Workshop on Degradation Issues in Fuel Cells, Greece, September 19–21, 2007.
[87] J. Sfeir, Alternative anode materials for methane oxidation in solid oxide fuel cells, Thesis N6446, EPFL Lausanne, 2001.
[88] M. Gong, X. Liu, J. Trembly, C. Johnson, J. Power Sources 168 (2) (2007) 289–298.
[89] Y. Matsuzaki, I. Yasuda, Solid State Ionics 132 (2000) 261–269.
[90] M. Mogensen, K.V. Jensen, Solid State Ionics 150 (2002) 123–129.
[91] K.V. Jensen, R. Wallenberg, I. Chorkendorff, M. Mogensen, Solid State Ionics 160 (2003) 27–37.
[92] Y.L. Liu, S. Primdahl, M. Mogensen, Solid State Ionics 161 (2003) 1–10.
[93] Y.L. Liu, C. Jiao, Solid State Ionics 176 (2005) 435–442.
[94] S. Koch, P.V. Hendriksen, M. Mogensen, Y.L. Liu, N. Dekker, B. Rietveld, B. de Haart, F. Tietz, Fuel Cells 06 (2) (2006) 130–136.
[95] A. Gubner, H. Landes, J. Metzger, H. Seeg, R. Stübner, in: U. Stimming, S.C. Singhal, H. Tagawa, W. Lehnert (Eds.), Solid Oxide Fuel Cells V (SOFC-V), The Electrochemical Society, Pennington, USA, 1997, pp. 844–850, PV97-18.
[96] A. Müller, Mehrschicht-Anode für die Hochtemperaturbrennstoffzelle (SOFC), Thesis, University Karlsruhe, 2004.
[97] D.W. Dees, T.D. Claar, T.E. Easler, D.C. Fee, F.C. Mrazek, J. Electrochem. Soc. 134 (9) (1987) 2141–2146.
[98] M. Guillodo, P. Vernoux, J. Fouletier, Solid State Ionics 127 (2000) 99–107.
[99] S.P. Jiang, J.G. Love, L. Apateanu, Solid State Ionics 160 (2003) 15–26.
[100] M. Brown, S. Primdahl, M. Mogensen, J. Electrochem. Soc. 147 (2) (2000) 475–485.
[101] S. Primdahl, M. Mogensen, J. Electrochem. Soc. 144 (10) (1997) 3409–3419.
[102] S. Primdahl, M. Mogensen, J. Electrochem. Soc. 146 (8) (1999) 2827–2833.
[103] S. Primdahl, Y.L. Liu, J. Electrochem. Soc. 149 (11) (2002) A1466–A1472.

[104] A. Bieberle, The Electrochemistry of Solid Oxide Fuel Cell Anodes: Experiments, Modeling, and Simulations, Thesis, ETH Zurich, 2000.
[105] J. Hoffmann, M. Woski, R. Denzler, B. Doggwiler, T. Doerk, in: S.C. Singhal, J. Mizusaki (Eds.), Solid Oxide Fuel Cells IX (SOFC-IX), The Electrochemical Society, Pennington, USA, 2005, pp. 177–183, PV 2005-07.
[106] P. Haasen, Physikalische Metallkunde, Springer, Berlin-Heidelberg, New York, 1974, pp. 208–210.
[107] G. Robert, A. Kaiser, K. Honegger, E. Batawi, 5th European Solid Oxide Fuel Cell Forum, Lucerne, 2002, pp. 116–122.
[108] J. Abel, A.A. Kornyshev, W. Lehnert, J. Electrochem. Soc. 144 (12) (1997) 4253–4259.
[109] J. Sehested, J.A.P. Gelten, I.N. Remediakis, H. Bengaard, J.K. Norskov, J. Catal. 223 (2004) 432–443.
[110] J. Sehested, J.A.P. Gelten, S. Helveg, Appl. Catal. A: Gen. 309 (2006) 237–246.
[111] J. Sehested, J. Catal. 217 (2003) 417–426.
[112] J. Sehested, Catal. Today 111 (2006) 103–110.
[113] W. Fischer, J. Malzbender, G. Blass, R.W. Steinbrech, J. Power Sources 150 (2005) 73–77.
[114] J. Malzbender, T. Wakui, R.W. Steinbrech, Fuel Cells 06 (2) (2006) 123–129.
[115] A.G. Evans, J. Am. Ceram. Soc. 65 (10) (1982) 497–501.
[116] M. Mori, T. Yamamoto, H. Itoh, H. Inaba, H. Tagawa, J. Electrochem. Soc. 145 (4) (1998) 1374–1381.
[117] T. Klemensø, C. Chung, P.H. Larsen, M. Mogensen, J. Electrochem. Soc. 152 (11) (2005) A2186–A2192.
[118] G. Robert, A. Kaiser, E. Batawi, 6th European Solid Oxide Fuel Cell Forum, Lucerne, 2004, pp. 193–199.
[119] D. Fouquet, A.C. Müller, A. Weber, E. Ivers-Tiffée, Ionics 8 (2003) 103–108.
[120] J. Pusz, A. Smirnova, A. Mohammadi, N.M. Sammes, J. Power Sources 163 (2007) 900–906.
[121] T. Klemensø, C.C. Appel, M. Mogensen, Electrochem. Solid State Lett. 9 (9) (2006) A403–A407.
[122] G. Robert, A.F.J. Kaiser, E. Batawi, EP1513214A1, 2004.
[123] G. Robert, A.F.J. Kaiser, E. Batawi, EP1596458A1, 2005.
[124] G. Robert, A.F.J. Kaiser, E. Batawi, US 2003/0165726 A1, 2003.
[125] N.M. Tikekar, T.J. Armstrong, A.V. Virkar, J. Electrochem. Soc. 153 (4) (2006) A654–A663.
[126] J.L. Young, V. Vedahara, S. Kung, S. Xia, V.I. Briss, ECS Trans. 7 (1) (2007) 1511–1519.
[127] K. Kendall, C.M. Dikwal, W. Bujalski, ECS Trans. 7 (1) (2007) 1521–1526.
[128] S. Tao, J.T.S. Irvine, Nat. Mater. 2 (2003) 320–323.
[129] O.A. Marina, J.S. Hardy, G.W. Coffey, S.P. Simmer, K.D. Meinhardt, All-Ceramic Sofc Tolerant To Oxygen, Carbon And Sulphur, Fuel Cell Seminar 2002, Palm Springs, 2002.
[130] A. Mitterdorfer, L.J. Gauckler, Solid State Ionics 111 (1998) 185–218.
[131] M.J. Heneka, E. Ivers-Tiffée, in: S. Linderoth, A. Smith, N. Bonanos, A. Hagen, L. Mikkelsen, K. Kammer, D. Lybye, P.V. Hendriksen, F.W. Poulsen, M. Mogensen, W.G. Wang (Eds.), Proceedings of the 26th Risø International Symposium on Materials Science, Risø National Laboratory, Roskilde, Denmark, 2005, pp. 215–222.
[132] H. Timmermann, Presentation at the International Workshop on Degradation Issues in Fuel Cell, Heronissos, Greece, September 19–21, 2007.
[133] A. Hagen, R. Barfod, P.V. Hendriksen, Y.-L. Liu, S. Ramousse, J. Electrochem. Soc. 153 (2006) A1165–A1171.
[134] T. Kawada, N. Sakai, H. Yokokawa, M. Dokiya, Solid State Ionics 53–56 (1992) 418–425.
[135] S. Ziesche, N. Trofimenko, M. Kuznecov, W. Preidel, in: S. Linderoth, A. Smith, N. Bonanos, A. Hagen, L. Mikkelsen, K. Kammer, D. Lybye, P.V. Hendriksen, F.W. Poulsen, M. Mogensen, W.G. Wang (Eds.), Proceedings of the 26th Risø International Symposium on Materials Science, Risø National Laboratory, Roskilde, Denmark, 2005, pp. 375–382.
[136] L.G.J. de Haart, I.C. Vinke, A. Janke, H. Ringel, F. Tietz, in: H. Yokokawa, S.C. Singhal (Eds.), Solid Oxide Fuel Cells VII, (SOFC-VII), The Electrochemical Society, Pennington, USA, 2001, pp. 111–119, PV2001-16.
[137] S.P. Simner, M.D. Anderson, M.H. Engelhard, J.W. Stevenson, Electrochem. Solid-State Lett. 9 (2006) A478–A481.
[138] G. Orsello, G. Disegna, K. Litzinger, R. Basel, M. Cali, M. Santrelli, Proceedings of the 7th European SOFC Forum European Fuel Cell Forum, Oberrohrdorf, Switzerland, 2006, File No. A071.
[139] A. Mai, V.A.C. Haanappel, S. Uhlenbruck, F. Tietz, D. Stöver, Solid State Ionics 176 (2005) 1341–1350.
[140] N. Sakai, H. Kishimoto, K. Yamaji, T. Horita, M.E. Brito, H. Yokokawa, in: K. Eguchi, S.C. Singhal, H. Yokokawa, J. Mizusaki (Eds.), Solid Oxide Fuel Cells 10 (SOFC-X), The Electrochemical Society, Pennington, USA, ECS Trans. 7 (2007) 389–398.
[141] M. Becker, Ph.D. Thesis, University Karlsruhe, Germany, 2007 (in German).
[142] A. Mai, V.A.C. Haanappel, F. Tietz, D. Stöver, Solid State Ionics 177 (2006) 2103–2107.
[143] V.A.C. Haanappel, A. Mai, J. Mertens, Solid State Ionics 177 (2006) 2033–2037.
[144] S. Koch, M. Mogensen, P.V. Hendriksen, N. Dekker, B. Rietveld, Proceedings of the 6th European SOFC Forum, European Fuel Cell Forum, Oberrohrdorf, Switzerland, 2004, pp. 1000–1009.
[145] A. Mai, F. Tietz, D. Stöver, Final report on the BMBF-project "Neue katalytisch aktive Kathodenwerkstoffe für SOFCs mit abgesenkter Betriebstemperatur" (in German), available online at http://edok01.tib.uni-hannover.de/edoks/e01fb07/523372957.pdf.
[146] F. Tietz, A. Mai, D. Stöver, Solid State Ionics (2008), doi:10.1016/j.ssi.2007.11.037, in press.
[147] F. Tietz, Q. Fu, V.A.C. Haanappel, A. Mai, N.H. Menzler, S. Uhlenbruck, Int. J. Appl. Ceram. Technol. 4 (2007) 436–445.
[148] S.P. Simner, M.D. Anderson, G.-G. Xia, Z. Yang, L.R. Pederson, J.W. Stevenson, J. Electrochem. Soc. 152 (2005) A740–A745.
[149] E. Konysheva, H. Penkalla, E. Wessel, J. Mertens, U. Seeling, L. Singheiser, K. Hilpert, J. Electrochem. Soc. 153 (2006) A765–A773.
[150] J.-Y. Kim, V.L. Sprenkle, N.L. Canfield, K.D. Meinhardt, L.A. Chick, J. Electrochem. Soc. 153 (2006) A880–A886.
[151] A. Mai, V.A.C. Haanappel, F. Tietz, D. Stöver, in: S.C. Singhal, J. Mizusaki (Eds.), Solid Oxide Fuel Cells IX (SOFC-IX), The Electrochemical Society, Pennington, USA, 2005, pp. 1627–1635.
[152] S.P. Simner, J.R. Bonnett, N.L. Canfield, K.D. Meinhardt, J.P. Shelton, V.L. Sprenkle, J.W. Stevenson, J. Power Sources 113 (2003) 1–10.
[153] M.D. Anderson, J.W. Stevenson, S.P. Simner, J. Power Sources 129 (2004) 188–192.
[154] S.P. Simner, M.D. Anderson, L.R. Pederson, J.W. Stevenson, J. Electrochem. Soc. 152 (2005) A1851–A1859.
[155] C. Lalanne, F. Mauvy, J.-M. Bassat, J.-C. Grenier, P. Stevens, G. Prosperi, J. Van herle, S. Diethelm, R. Ihringer, Proceedings of the 7th European SOFC Forum, European Fuel Cell Forum, Oberrohrdorf, Switzerland, 2006, File No. B063.
[156] H. Orui, K. Watanabe, R. Chiba, M. Arakawa, J. Electrochem. Soc. 151 (2004) A1412–A1417.